Planta (2020) 252:32
https://doi.org/10.1007/s00425-020-03439-6

ORIGINAL ARTICLE

Spatio–temporal immunolocalization of extensin protein and hemicellulose polysaccharides during olive fruit abscission

Ruben Parra[1] · **Maria C. Gomez-Jimenez**[1]

Received: 27 May 2020 / Accepted: 29 July 2020 / Published online: 5 August 2020

Abstract

Main conclusion **Immunocytochemical and molecular analyses reveal that the disassembly of the cell wall may be mediated by changes in the level and subcellular location of extensin protein and hemicelluloses during olive-fruit abscission.**

Abstract Although cell-wall modification is believed to underlie the changes in organ abscission, information concerning the changes in cell-wall proteins and hemicellulose polysaccharides is still limited. The aim of this work was to analyze the spatio–temporal patterns of the distribution of different extensin proteins and hemicelluloses in the abscission zone (AZ) during natural ripe-fruit abscission in olive (*Olea europaea* L.). In this study, we employed immunogold labeling in the ripe-fruit AZ during olive AZ cell separation, using an expanded set of monoclonal antibodies that recognize different types of hemicelluloses (LM11, LM15, and LM21), callose (anti-(1,3)-β-D-glucan) and extensin (JIM19) epitopes, and transmission electron microscopy imaging. Our data demonstrate that AZ cell separation was accompanied by a loss of the JIM19 extensin epitopes and a reduction in the detection of the LM15 xyloglucan epitopes in AZ cell walls, whereas AZ cells were found to be enriched with respect to the xylan and callose levels of the cell wall during olive ripe-fruit abscission. By contrast, AZ cell-wall polysaccharide remodeling did not involve mannans. Moreover, in ripe-fruit AZ, quantitative RT-PCR analysis revealed that *OeEXT1*, *OeEXT2*, *OeXTH9*, and *OeXTH13* genes were downregulated during abscission, whereas the expression of *OeXTH1*, *OeXTH5*, and *OeXTH14 g*enes increased during abscission. Taken together, the results indicate that AZ cell-wall dynamics during olive ripe-fruit abscission involves extensin protein and hemicellulose modifications, as well as related expressed genes. This is the first study available demonstrating temporal degradation of extensin protein and hemicelluloses in the AZ at the subcellular level.

Keywords Callose · Cell wall · Extensin protein · Fruit abscission · Hemicellulose · Immunolocalization

Abbreviations

AGP	Arabinogalactan protein
AZ	Abscission zone
DPA	Days post-anthesis
EGase	Endo-β-1,4-glucanase
EXP	Expansin
XET	Xyloglucan endotransglucosylase
XTH	Xyloglucan endotransglucosylase-hydrolase

Communicated by Anastasios Melis.

Electronic supplementary material The online version of this article (https://doi.org/10.1007/s00425-020-03439-6) contains supplementary material, which is available to authorized users.

✉ Maria C. Gomez-Jimenez
mcgomez@unex.es

[1] Department of Plant Physiology, Faculty of Science, University of Extremadura, Avda de Elvas s/n, 06006 Badajoz, Spain

Introduction

Organ abscission involves numerous modifications to the abscission zone (AZ) cell wall, a structure composed of polysaccharides (mainly pectin, hemicellulose, and cellulose), as well as structural and polysaccharide-modifying proteins, and this composition differs between different plant species (Wolf et al. 2012; Voiniciuc et al. 2018). Because pectins are the major structural components of the middle lamella at intercellular junctions and the corners of intercellular spaces, where they contribute to

cell separation (Bouton et al. 2002; McCartney and Knox 2002; Caffall and Mohnen 2009; Wolf et al. 2009; Levesque-Tremblay et al. 2015; Voiniciuc et al. 2018), the pectin content of the AZ cell walls has received special attention regarding composition and dynamics of their components during the abscission process (Uheda and Nakamura 2000; Lee et al. 2008, 2016; Bowling and Vaughn 2011; Iwai et al. 2013; Tsuchiya et al. 2015; Roongsattham et al. 2016; Merelo et al. 2017; Parra et al. 2020). However, the dynamics of other components of AZ cell wall, such as the hemicellulose, has been left behind. Hemicelluloses are estimated to account for about one third of all components available in plants and are the second heteropolymers present in nature (Chaikumpollert et al. 2004). Hemicellulose polysaccharides are structurally diverse, including xyloglucans, xylans, and mannans (O'Neill and York 2003; Liepman et al. 2007), which are involved in the cross-linking of cellulose microfibrils (Scheller and Ulvskov 2010; Palmer et al. 2015). Xyloglucan is the predominant hemicellulose in the primary cell walls of nongraminaceous species (Cosgrove 1997; Pauly and Keegstra 2016; Voiniciuc et al. 2018) and it functions as a tether between cellulose microfibrils (Carpita and Gibeaut 1993; Marcus et al. 2008; Hayashi and Kaida 2011). Meanwhile, xylans and mannans are the two major classes of hemicelluloses that accumulate in secondary cell walls but are also components of primary walls of dicots (Hervé et al. 2009; Scheller and Ulvskov 2010; Mortimer et al. 2015; Voiniciuc et al. 2018). Although advanced techniques to monitor hemicellulose polysaccharides with the genomics data have identified hemicellulose metabolism-related genes involved in the abscission process (Tucker et al. 2007; Agustí et al. 2008; Merelo et al. 2017; Cai and Lashbrook 2008; Meir et al. 2010; Singh et al. 2011; Corbacho et al. 2013; Li et al. 2015; Tsuchiya et al. 2015; Glazinska et al. 2017), the spatio–temporal organization, and the regulation of AZ cell-wall hemicellulose synthesis and degradation, as well as the dynamics of AZ cell-wall assemblies during organ abscission, remain unclear. In particular, the dynamics of mannan, using immunocytochemistry method, have yet to be explored in organ abscission, and, to date, only a few studies have provided information on the degradation of xyloglucan and xylan polysaccharides in AZ cell walls (Lee et al. 2008; Iwai et al. 2013; Tsuchiya et al. 2015). In poinsettia, at a late stage of floral abscission, xylan and xyloglucan epitopes have been shown to be present together with lignin around the AZ and in distal tissues using immunohistochemistry (Lee et al. 2008). Similarly, in tomato, an increase has been observed in LM15 labeling of xyloglucan specifically at the AZ during floral abscission, but not at the AZ during ripe-fruit abscission, suggesting that floral abscission and fruit abscission, which occurs post-ripening, are regulated by different mechanisms. Floral abscission occurs through the remodeling of cell-wall polysaccharides, and fruit abscission through lignification (Iwai et al. 2013).

The hemicellulosic components of the plant cell wall include a variety of polysaccharides with linear or branched polymers derived from sugars such as D-xylose, D-galactose, D-mannose, D-glucose, and L-arabinose (Voiniciuc et al. 2018). The degradation of hemicellulose structures involves the concerted action of a variety of hydrolytic enzymes (Voiniciuc et al. 2018). In the enzymatic disassembly of hemicellulose polysaccharides, the involvement of xyloglucan endotransglucosylase-hydrolase (XTH), endo-β-1,4-glucanase (EGase) and expansin (EXP) have been investigated in organ abscission (Roberts et al. 2002; Belfield et al. 2005; Tucker et al. 2007; Agustí et al. 2008; Cai and Lashbrook 2008; Singh et al. 2011; Tsuchiya et al. 2015). During rose-petal abscission, it has been shown that cell-wall remodeling of the xyloglucan moieties through the xyloglucan endotransglucosylase (XET) action of XTHs may be key for cell separation (Singh et al. 2011). The pattern of xyloglucan degrading enzyme activity in abscission is apparently complex (Singh et al. 2011; Tsuchiya et al. 2015; Prakash et al. 2017) and may reflect a combination of hydrolases, transglucosylases, and/or enzymes with both activities.

Among the AZ cell-wall proteins, AGPs and extensins are major members of the plant cell-wall hydroxyproline-rich glycoproteins (HRGPs) superfamily and recent findings suggest that wall ion-regulated intermolecular interaction/adhesions between AGPs and/or extensins may be involved in maintaining wall–plasma membrane integrity during cell-wall loosening processes such as cell-wall expansion (Tan et al. 2018). AGPs are a constituent of floral AZs during and soon after complete cell separation in Arabidopsis (Stenvik et al. 2006; Seifert and Roberts 2007; Cho et al. 2008), however, the role of cell-wall extensin proteins in abscission processes is comparatively less known. Extensins, like AGPs, are important in plant growth, development, and defense (Lamport et al. 2011; Saha et al. 2013; Liu et al. 2016; Showalter and Basu 2016; Doll et al. 2020; Zdanio et al. 2020). Previously, the preferential accumulation of SAC5, a proline-rich protein, has been shown in the dehiscence zone of the oilseed ripe pod (Coupe et al. 1993). In Arabidopsis, the extensin gene *atext1*, induced by a variety of biotic and abiotic stresses, is expressed in AZ during floral abscission (Merkouropoulos and Shirsat 2003). Nevertheless, to date, the dynamics of extensin, using immunocytochemistry method, have yet to be thoroughly investigated in the abscission process.

Olive (*Olea europaea* L), one of the most economically important fruit trees worldwide, includes such cultivars as 'Picual', which undergoes massive natural fruit abscission

after fruit ripening (Gomez-Jimenez et al. 2010a). For this and other cultivars, applications of ethephon or 1-aminocyclopropane-1-carboxylate (ACC) promote fruit abscission (Barranco et al. 2004; Burns et al. 2008; Parra-Lobato and Gomez-Jimenez 2011). In general, fleshy-fruit abscission after ripening is a genetically programmed process (Périn et al. 2002), and a developmentally controlled program of cell separation that occurs through the dissolution of AZ cell walls (Bleecker and Patterson 1997; Patterson 2001; Roberts et al. 2002; McManus 2008; Niederhuth et al. 2013; Patharkar and Walker 2018; Meir et al. 2019). The presence of the AZ is an agronomically important trait in many species in terms of the ease of fruit detachment at harvest (Roberts et al. 2002; Xie et al. 2013; Patharkar and Walker 2018; Meir et al. 2019; Tranbarger and Tadeo 2020). The olive fruit, like other fleshy-fruit, has several AZs in the pedicel (Bartolini et al. 1993), but only one AZ (i.e. located between the pedicel and fruit), is selectively activated after fruit ripening (Gomez-Jimenez et al. 2010a; Parra-Lobato and Gomez-Jimenez 2011). In a previous study, we reported on the comparison of the Picual fruit AZ transcriptomes at two different stages during AZ cell separation (pre-abscission vs. abscission) using the RNA-Seq technique (Gil-Amado and Gomez-Jimenez 2013). Among the differentially expressed genes in the olive AZ during ripe-fruit abscission, we have identified several genes involved in cell-wall metabolism (Gil-Amado and Gomez-Jimenez 2013), indicating that this process of cell-wall disassembly requires many enzymes acting in concert. Recently, we have demonstrated that the changes detected in AZ cell-wall polysaccharides during olive ripe-fruit abscission are related to pectic polysaccharide de-esterification and solubilization (Parra et al. 2020). In olive-fruit AZ, abscission is associated with an increase of de-esterified pectins, by the detection of the LM19 homogalacturonan epitope, mainly in the middle lamella and cellular junctions (Parra et al. 2020). Likewise, the abundance of the highly methylesterified homogalacturonan epitope recognized by the LM20 antibody diminished during olive ripe-fruit abscission, as did the abundance of LM5 for 1,4-galactan and LM6 for 1,5-arabinan (Parra et al. 2020). In addition, sugar compositional analyses in the olive AZ of both stages showed that the sugar composition of noncellulosic monosaccharide residues in the AZ cell-wall material was different during abscission (Parra et al. 2020), but the dynamics of hemicelluloses have yet to be explored using immunocytochemistry in olive-fruit abscission.

In the present study, we performed a detailed analysis of the changes in AZ cell-wall hemicelluloses at spatio–temporal pattern during olive ripe-fruit abscission. We used immunogold labeling to study the distribution of hemicelluloses (including xyloglucan, xylan, and mannan), extensin, and callose epitopes in the fruit AZ, quantifying and comparing their relative levels and subcellular location during olive-fruit AZ cell separation. In addition, we explored the transcriptional regulation of genes that encode XTH (*OeXTH1*, *OeXTH5*, *OeXTH9*, *OeXTH13,* and *OeXTH14*) and extensin (*OeEXT1* and *OeEXT2*) proteins in the ripe-fruit AZ during abscission in olive.

Materials and methods

Plant material

Three trees of olive (*Olea europaea* L. cultivar 'Picual') that entered full bloom on the same day were selected from an orchard located in Badajoz (Spain). This olive cultivar exhibits massive natural fruit abscission after ripening, and ripe-fruit abscission occurs in the pedicel-fruit AZ (Gomez-Jimenez et al. 2010a; Parra-Lobato and Gomez-Jimenez 2011). Olive flowers were tagged on the day of pollination and the AZ samples were collected from olive fruits subsequently harvested at two specified stages during ripe-fruit AZ cell separation: pre-abscission (unseparated AZ cells) and abscission (partially separated AZ cells) stages (Gil-Amado and Gomez-Jimenez 2013; Parra-Lobato et al. 2017; Parra et al. 2020). Fruit AZs from three trees were collected in the seasons 2016 and 2017 at the two stages. At each stage, 150 fruit AZs per tree were collected for analysis. Fruit AZ from each tree formed a biological replicate. The fruit AZs were manually dissected from longitudinal sections of the samples with a razor blade into pieces to a maximum width of 1 mm on each side of the abscission fracture plane (Gil-Amado and Gomez-Jimenez 2013; Parra-Lobato et al. 2017; Parra et al. 2020). Fruit AZ samples containing mesocarp or pedicel/calyx-like tissues were discarded (Parra et al. 2013). For the cytological study, five fruit AZs per tree were collected at each stage, cut into pieces approximately 0.3–0.6 mm thick, and rapidly fixed for 2 h in ethanol-acetic acid (3:1, v/v) at room temperature. The samples were rinsed three times in 70% ethanol, dehydrated by an ethanol series, and embedded in Technovit 7100 (Kulzer). Sections (1 mm) made with glass knives were stained with 0.04% (w/v) toluidine blue and photographed using a Zeiss Axiophot microscope coupled to a Spot digital camera (Diagnostic Instruments) (Fig. 1).

Immunogold labeling

All immunocytochemistry experiments were performed using multiple sections taken from embedded AZ tissue for each stage from three biological replicates. At each stage, five fruit AZs per tree were examined per replicate ($n = 15$). Freshly excised AZ samples at two stages (pre-abscission and abscission) were fixed in 4% (w/v) paraformaldehyde and 0.25% (w/v) glutaraldehyde in 0.1 M phosphate buffer

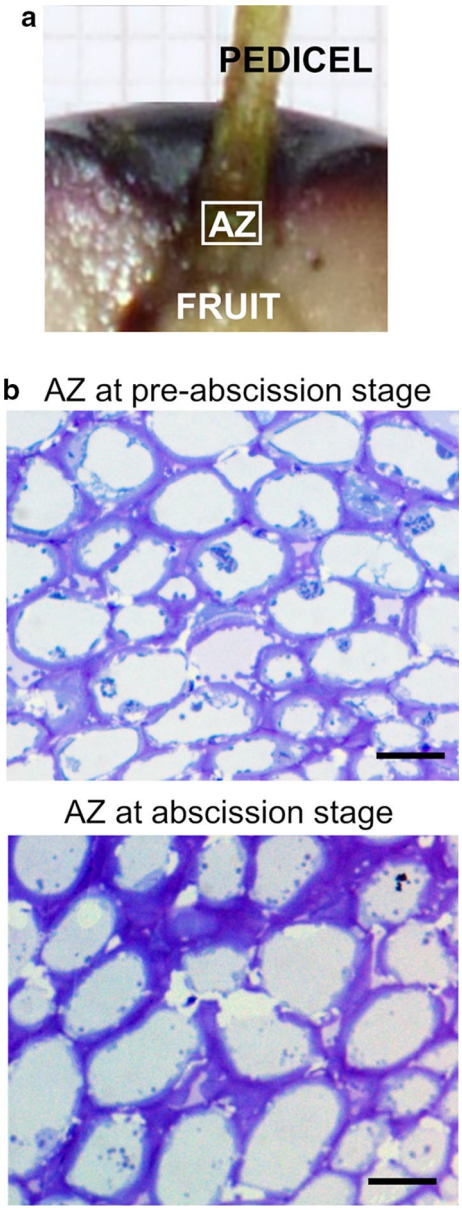

Fig. 1 Tissues of olive (*Olea europaea* L. cv Picual) used for this study. **a** Longitudinal section of the transition zone between the pedicel (top) and fruit (bottom) showing the AZ of olive ripe-fruit. **b** Longitudinal sections of the ripe-fruit AZ at the pre-abscission (unseparated AZ cells), and abscission (partially separated AZ cells) stages were stained with toluidine blue. Scale bars 15 µm in **b**

(pH 7.2), and placed under vacuum for 1 h and then at 4 °C overnight. After dehydration in a graded ethanol series, the material was embedded in LR White resin, as described by Olmos et al. (2017). Ultrathin sections (70 nm) were made with a Leica EM UC6 ultramicrotome (Leica Mycrosystems, Hernalser Hauptstraße, Vienna, Austria) and collected on formvar-coated nickel grids. The grids were placed in phosphate-buffered saline (PBS) with 5% bovine serum albumin (BSA) for 30 min at room temperature and then incubated for 2 h with the primary monoclonal antibodies diluted (1:5) in PBS containing 5% BSA. The primary antibodies used were JIM19 (extensin), LM11 (xylan), LM15 (xyloglucan), and LM21 (mannan) from PlantProbes (Leeds, UK), and anti-1,3-β-glucan (callose) from Biosupplies (Parkville, VIC, Australia). The sections were washed three times in PBS and incubated with the secondary antibody (goat anti-rat coupled with 15-nm colloidal gold, BioCell International) diluted 1:50 in PBS supplemented with 1% BSA. The grids were washed in buffer and distilled water and dried at 37 °C. Controls were run every time for each of the antibodies by omitting incubation with the primary antibody (Supplementary Fig. S1). Samples were examined using a TEM TECNAI G2 20 Twin transmission electron microscope.

Quantitative analysis of immunogold labeling

The images were captured directly with a CCD SIS MegaView camera and then analyzed by means of the software AnalySIS® version 3.0. (Soft Imaging System GmbH, Münster, Germany). The software AnalySIS®Gold was used for manually identifying the particles. Also, the cell-wall area, the plasma-membrane length, and the cytoplasm were measured manually using the software AnalySIS®. The statistical analysis included an examination of at least 3 different AZs per stage and per antibody. For the statistical treatment of the data, the software Statistix 8 (NH Analytical Software, Roseville, MN, USA) was used, and the statistical differences were analyzed using the unpaired Student's *t* test ($p < 0.05$).

Quantitative RT-PCR

Previously published RNA-Seq data (Gil-Amado and Gomez-Jimenez 2013), were mined for cell-wall remodeling-related genes. Expression levels were determined for genes encoding the extensin (*OeEXT1, OeEXT2*), and XTH (*OeXTH1*, *OeXTH5*, *OeXTH9*, *OeXTH1,* and *OeXTH14;* EC:2.4.1.207) proteins. The sequences were confirmed and deposited in the GenBank database (Supplementary Data Table S1). The phylogenetic analysis was performed by comparing the conserved domains of EXT (Supplementary Fig. S2), and XTH (Supplementary Fig. S3) sequences from our work and Arabidopsis (https://www.arabidopsis.org/). Total RNA (2 µg) was reverse transcribed with random hexamers and Superscript III (Invitrogen), according to the manufacturer's instructions. Purified cDNA (2 ng) was used as a template for quantitative RT-PCR (qRT-PCR). qRT-PCR assays were performed with gene-specific primers (Supplementary Data Table S1). The cDNA was amplified using a SYBRGreen-PCR Master kit (Applied Biosystems) containing an AmpliTaq Gold polymerase on an iCycler (BioRad Munich), following the protocol provided by the supplier. Samples were subjected to thermal cycling conditions of

DNA polymerase activation at 94 °C, 45 s at 55 °C, 45 s at 72 °C, and 45 s at 80 °C; a final elongation step of 7 min at 72 °C was performed. The melting curve was designed to increase by 0.5 °C every 10 s from 62 °C. The amplicon was analyzed by electrophoresis and sequenced once for confirmation of identity. qRT-PCR efficiency was estimated via a calibration dilution curve and slope calculation. Expression levels were determined as the number of cycles needed for the amplification to reach a threshold fixed in the exponential phase of the PCR (CT). The data were normalized for the quantity of the *Olea europaea* ubiquitin (*OeUB*) gene (Gomez-Jimenez et al. 2010b). For each sample, three biological replicates with three technical repeats each were analyzed. Each biological replicate corresponds to pooled AZs from each tree.

Phylogenetic analysis

Phylogenetic trees were constructed based on similarity searches performed with BLASTp programs with default parameters in protein sequence databases provided by the National Center for Biotechnology Information server (http://www.ncbi.nlm.nih.gov). Amino acid sequences were aligned with ClustalW (version 2.0.3) (Thompson et al. 1994).

Accession numbers

Accession numbers for the genes studied in this work are: *OeEXT1* (MT753446), *OeEXT2* (MT753447), *OeXTH5* (MT753448), *OeXTH14* (MT753449), *OeXTH9* (MT753450), *OeXTH13* (MT753451), and *OeXTH1* (MT753452).

Statistical analysis

Significance analysis of corresponding experimental data was conducted using Statistix 8 software (NH Analytical Software, Roseville, MN, USA). Two-tailed Student's *t* test was performed to evaluate statistically significant differences between stages. The values $p < 0.05$ were considered statistically significant. For each sample, three independent biological replicates with at least three technical repeats each were analyzed.

Results

Immunolocalization of hemicelluloses in the fruit AZ during abscission

In 'Picual' olive, the ripe-fruit abscission depends on the activation of the AZ located between the pedicel and fruit (Fig. 1a). The fruit-detachment force significantly weakens during 'Picual' fruit ripening, coinciding with a peak content of 1-aminocyclopropane-1-carboxylic acid, an ethylene precursor, in the AZ at 217 days post-anthesis (DPA), at which time abscission occurs (Parra-Lobato and Gomez-Jimenez 2011). For this work, we selected the Picual fruit AZ tissue at two different stages during AZ cell separation: pre-abscission (unseparated AZ cells) and abscission (partially separated AZ cells). Initially, thin sections from each AZ at the two stages were labeled with toluidine blue (Fig. 1b). This showed major differences in AZ cell size between the two stages. Furthermore, under the light microscope, the intercellular spaces in the AZ at the abscission stage appeared larger than at the pre-abscission stage, indicating some loss of cell-to-cell adhesion at these points (Fig. 1b). As in our previous study (Parra et al. 2020), the olive AZ cells at the abscission stage appeared to be enlarged, and separated from each other, generating the abscission plane during ripe-fruit abscission.

The ultrastructural immunolocalization of different types of hemicellulose epitopes (LM11, LM15, and LM21) were analyzed by immunogold labeling in ripe-fruit AZ longitudinal sections at both stages (pre-abscission and abscission) during olive AZ cell separation. For the immunolocalization of xylans, we used LM11 monoclonal antibody which recognizes arabinoxylan and low-substituted xylans (McCartney et al. 2005). Probing the fruit AZ sections with LM11 indicated a higher density of labeling in the AZ cells at the abscission stage than that at the pre-abscission stage (Table 1). An examination of the labeling pattern at the ultrastructural level revealed labeling mainly in the cytoplasm (Fig. 2a–f). In the AZ cell wall, including the tricellular junction zones, our analysis indicated that the LM11 epitope was sparse, and we found no preferred location of this epitope in the middle lamella (Fig. 2a–f). Control reaction performed by omitting the incubation of AZ tissue sections with primary antibody showed no immunogold labeling (Supplementary Fig. S1). Thus, the LM11 epitope showed a notable increase in the olive AZ cells especially in the cytoplasm during ripe-fruit abscission.

Xyloglucan was detected using LM15, an antibody cross-reacting with the XXXG motif of xyloglucan (Marcus et al. 2008). In contrast to the LM11 epitope, the density of LM15 labeling decreased in olive AZ cells during ripe-fruit abscission (Table 1, Fig. 3a–f). In the AZ cells, low levels of labeling for LM15 were apparent with some labeling in the cell walls and within the cell walls, especially in the inner region close to the plasmalemma, but absent from the tricellular junctions (Fig. 3b, e). Immunogold labeling with LM15 antibody was very scarce in cytoplasm and vacuole, showing a higher density in AZ cells at pre-abscission stage in comparison with AZ cells at the abscission stage (Table 1, Fig. 3a–f). Negative controls showed no significant labeling

Table 1 Quantification of immunogold labeling with JIM19, LM11, LM15, and LM21 antibodies during olive ripe-fruit abscission

	Number of gold particles		
	Cell-wall (μm^2)	Cytoplasm (μm^2)	Vacuole (μm^2)
JIM19			
AZ at pre-abscission stage	1.58 ± 0.32*	11.45 ± 0.20*	0.24 ± 0.16
AZ at abscission stage	0.00 ± 0.00	0.00 ± 0.00	0.00 ± 0.00
LM11			
AZ at pre-abscission stage	0.35 ± 0.10	2.08 ± 0.15	0.76 ± 0.35
AZ at abscission stage	1.90 ± 0.12*	7.37 ± 0.31*	0.48 ± 0.27
LM15			
AZ at pre-abscission stage	3.49 ± 0.46*	0.59 ± 0.15*	0.46 ± 0.17*
AZ at abscission stage	1.06 ± 0.13	0.25 ± 0.18	0.22 ± 0.13
LM21			
AZ at pre-abscission stage	1.25 ± 0.26	2.12 ± 0.39	1.25 ± 0.43
AZ at abscission stage	1.48 ± 0.31	2.75 ± 0.58	1.04 ± 0.61

Data are means of fruit AZ ± SD ($n = 15$) of three biological replicates per stage and per antibody. Five fruit AZs from each tree formed a biological replicate. Statistically significant differences based on unpaired Student's t test at $p < 0.05$ are denoted by an asterisk

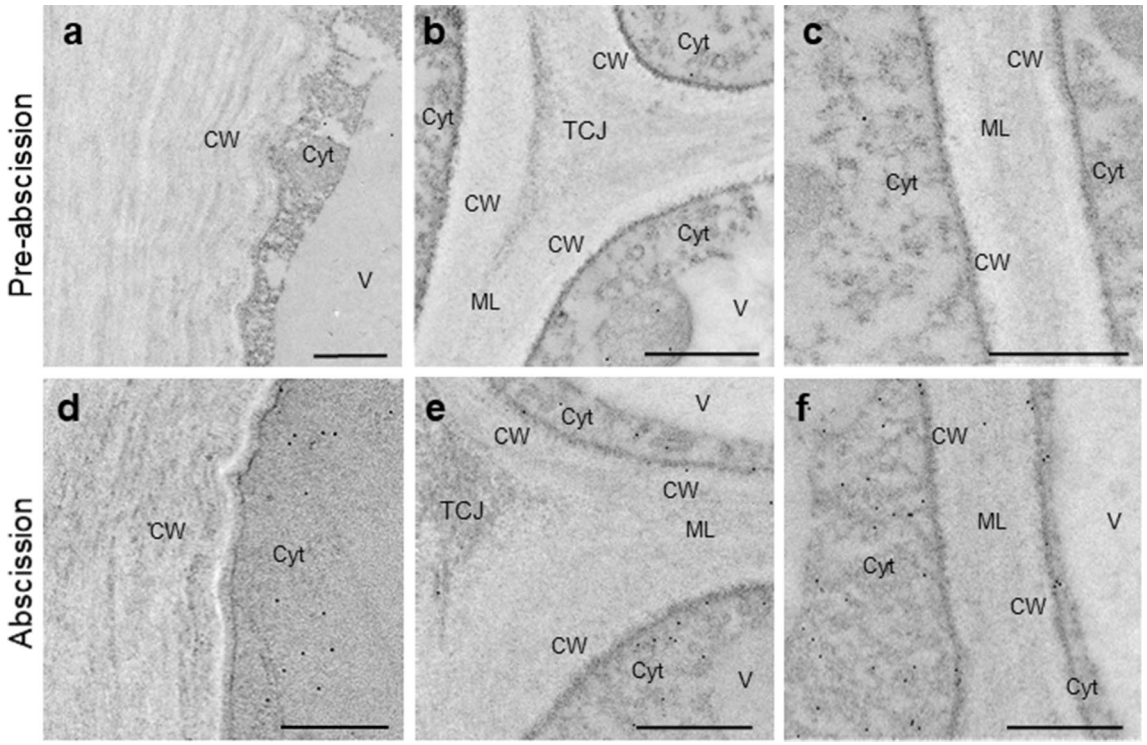

Fig. 2 Immunolocalization of xylan epitope (LM11) in the AZ cells during ripe-fruit abscission in olive (*Olea europaea* L. cultivar 'Picual'). Transmission electron micrographs of cell junctions from longitudinal sections of the fruit AZ at the **a**–**c** pre-abscission and **d**–**f** abscission stages. *CW* cell-wall, *cyt* cytoplasm, *ML* middle lamella, *TCJ* tricellular junction, *v* vacuole. Scale bars 1 µm

(Supplementary Fig. S1). Thus, the ripe-fruit abscission led to a decline of the LM15 xylan epitope in the olive AZ cell walls.

For the inmunolocalization of mannan epitopes within the AZ cells, we used the LM21 monoclonal antibody which is known to bind to heteromannans including glucomannan and galactomannan (Marcus et al. 2010). The density of LM21 mannan epitope labeling was relatively low and remained unchanged in the AZ cell during olive ripe-fruit abscission (Table 1, Fig. 4a–f). Incubation of ripe-fruit AZ

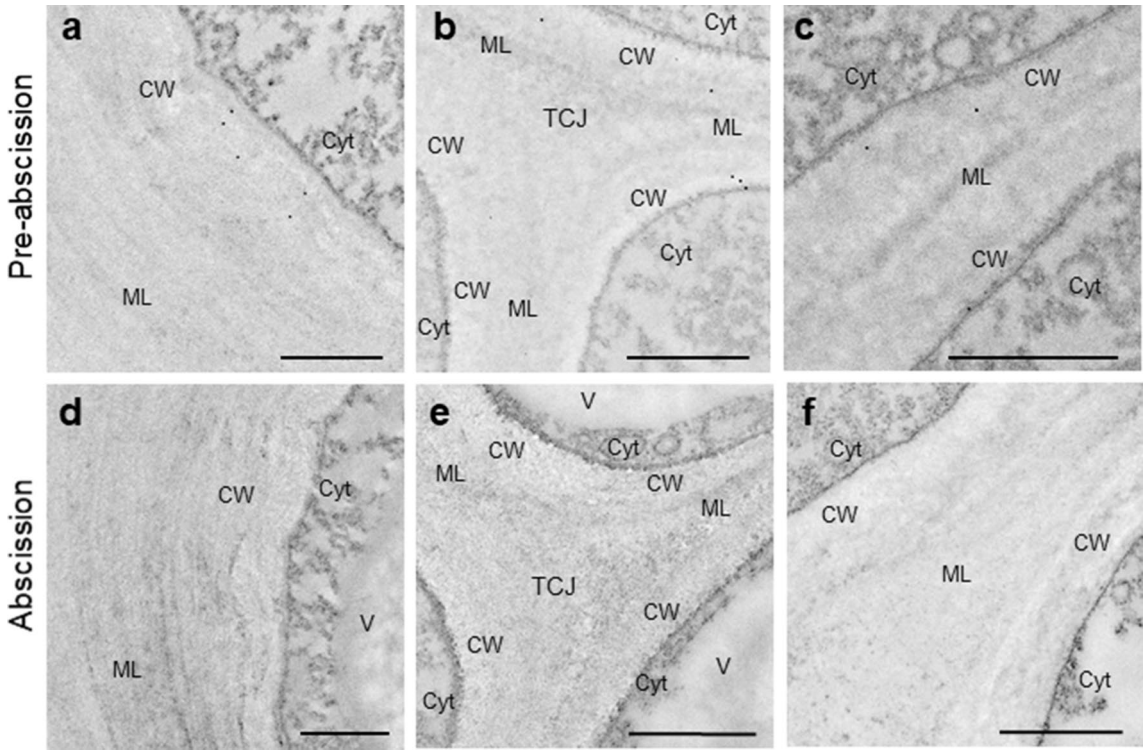

Fig. 3 Immunolocalization of xyloglucan epitope (LM15) in the AZ cells during ripe-fruit abscission in olive (*Olea europaea* L. cultivar 'Picual'). Transmission electron micrographs of cell junctions from longitudinal sections of the fruit AZ at the **a**–**c** pre-abscission and **d**–**f** abscission stages. *CW* cell-wall, *cyt* cytoplasm, *ML* middle lamella, *TCJ* tricellular junction, *v* vacuole. Scale bars 1 µm

sections with LM21 revealed that the cell walls were lightly labeled and that labeling was detectable mainly in the cytoplasm of the AZ cell at both stages (Fig. 4a–f). Negative controls showed no significant labeling (Supplementary Fig. S1). Thus, similar distribution of mannans in the AZ cells occurred during olive ripe-fruit abscission.

Immunolocalization of extensin protein in the AZ cells during olive-fruit abscission

Next, to investigate a relationship between the abscission process and the distribution of extensin protein in the ripe-fruit AZ, we located the JIM19 epitope using immunogold labeling in ripe-fruit AZ longitudinal sections at two different stages during olive AZ cell separation (pre-abscission and abscission stages). JIM19 showed the higher density of labeling in AZ cells at the pre-abscission stage in comparison with AZ cells at the abscission stage (Table 1, Fig. 5a–f). Our data indicated a complete absence of JIM19 labeling in the ripe-fruit AZ at the abscission stage (Fig. 5d–f). Ultrastructural localization of extensins in the olive AZ showed their presence in the cell wall and especially in the cytoplasm, but JIM19 labeling was absent from the cell junctions regions of AZ cells at both stages (Fig. 5a–f). Control reaction by omitting JIM19 showed no labeling after immunogold reaction (Supplementary Fig. S1). Hence, our data revealed a loss in extensin epitopes in the ripe-fruit AZ cells during abscission.

Immunolocalization of callose in the AZ cells during olive-fruit abscission

The presence of callose was determined using a (1,3)-β-D-glucan-specific monoclonal antibody (Meikle et al. 1991). The ultrastructural location of callose in the olive AZ showed its presence in the cell wall, the cytoplasm, and the plasmodesmatal connections on the cell wall (Fig. 6a, b, d, e), but callose labeling was absent from the tricellular junctions (Fig. 6c, f). The pattern of callose labeling changed in the AZ cells during ripe-fruit abscission (Fig. 6). At the pre-abscission stage, the epitope was found to be most abundant in the cytoplasm of the AZ cells, showing slightly higher density in AZ cells at pre-abscission in comparison with AZ cells at the abscission stage (Table 2, Fig. 6). By contrast, at the abscission stage, the epitope was more abundant in middle lamella region of the AZ cells, showing higher density in AZ cell walls at the abscission stage in comparison with AZ cell walls at the pre-abscission stage (Table 2, Fig. 6). Controls in which the primary antibody was omitted resulted in a complete lack of labeling (Supplementary Fig.

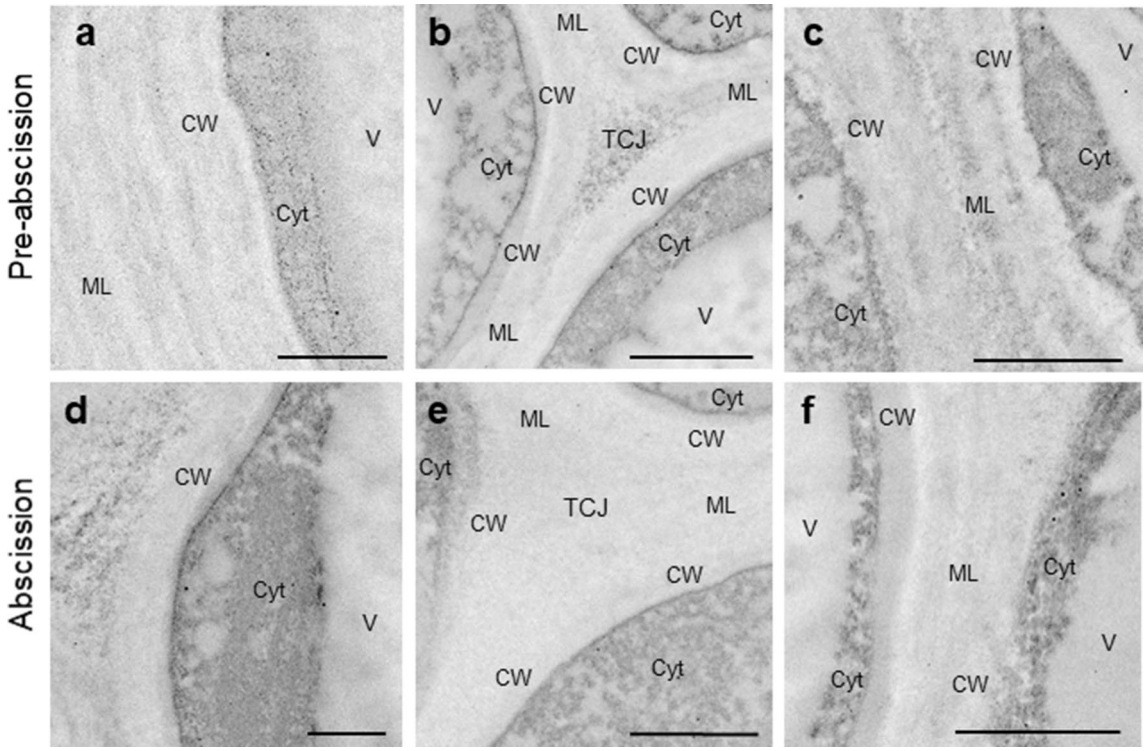

Fig. 4 Immunolocalization of mannan epitope (LM21) in the AZ cells during ripe-fruit abscission in olive (*Olea europaea* L. cultivar 'Picual'). Transmission electron micrographs of cell junctions from longitudinal sections of the fruit AZ at the **a**–**c** pre-abscission and **d**–**f** abscission stages. *CW* cell-wall, *cyt* cytoplasm, *ML* middle lamella, *TCJ* tricellular junction, *v* vacuole. Scale bars 1 µm

S1). Therefore, the level and distribution of callose in the AZ cells varies during olive ripe-fruit abscission.

Extensin and xyloglucan endotransglycosylase/hydrolase gene expression during olive-fruit abscission

To gain information concerning cell-wall dynamics during ripe-fruit abscission, we examined the expression of the genes encoding the extensin (*OeEXT1* and *OeEXT2*) and the XTH (*OeXTH1*, *OeXTH5*, *OeXTH9*, *OeXTH13,* and *OeXTH14*) proteins, as representative hemicellulose metabolism-related genes, in the olive-fruit AZ using qRT-PCR (Fig. 7; Supplementary Data Table S1, Fig. S2 and S3). The *OeXTH1*, *OeXTH5*, and *OeXTH14* transcript levels rose 7.7-, 8.5-, and 6.4-fold in the AZ at the abscission stage in comparison with those recorded in the AZ at the pre-abscission stage (Fig. 7), parallel to the xyloglucan level decrease (Fig. 3), whereas our data indicate that *OeXTH9* and *OeXTH13* were downregulated in the ripe-fruit AZ during abscission. The expression of *OeEXT1* and *OeEXT2* was also downregulated in the ripe-fruit AZ during abscission in association with lower extensin labeling density (Figs. 5, 7). Thus, ripe-fruit abscission induced the expression of *OeXTH1*, *OeXTH5*, and *OeXTH14* in the olive AZ, suggesting that these genes could be strongly associated with AZ cell separation during ripe-fruit abscission.

Discussion

Cell wall structural proteins and hemicellulosic matrix may be essential to the structural integrity of the cell wall, but to date few studies have shown the disassembly of hemicellulose in organ abscission processes. In particular, the subcellular location of these cell-wall components in the AZ remains to be determined. In the present study, with the use of immunogold labeling and transmission electron microscopy, changes in extensin and hemicellulose level and subcellular location were investigated in the AZ by comparing two stages (pre-abscission or unseparated AZ cells, and abscission or partially separated AZ cells) during ripe-fruit abscission in olive (*Olea europaea* L. cv. Picual). In addition, we investigated the relationship between extensin/hemicelluloses content and the expression of *OeEXT1*, *OeEXT2*, *OeXTH1*, *OeXTH5*, *OeXTH9*, *OeXTH13* and *OeXTH14* genes, using qRT-PCR, during olive ripe-fruit abscission.

Hemicellulose polysaccharides have not been widely found to be related to cell separation processes. In this study, the distribution of pattern of xylan and xyloglucan

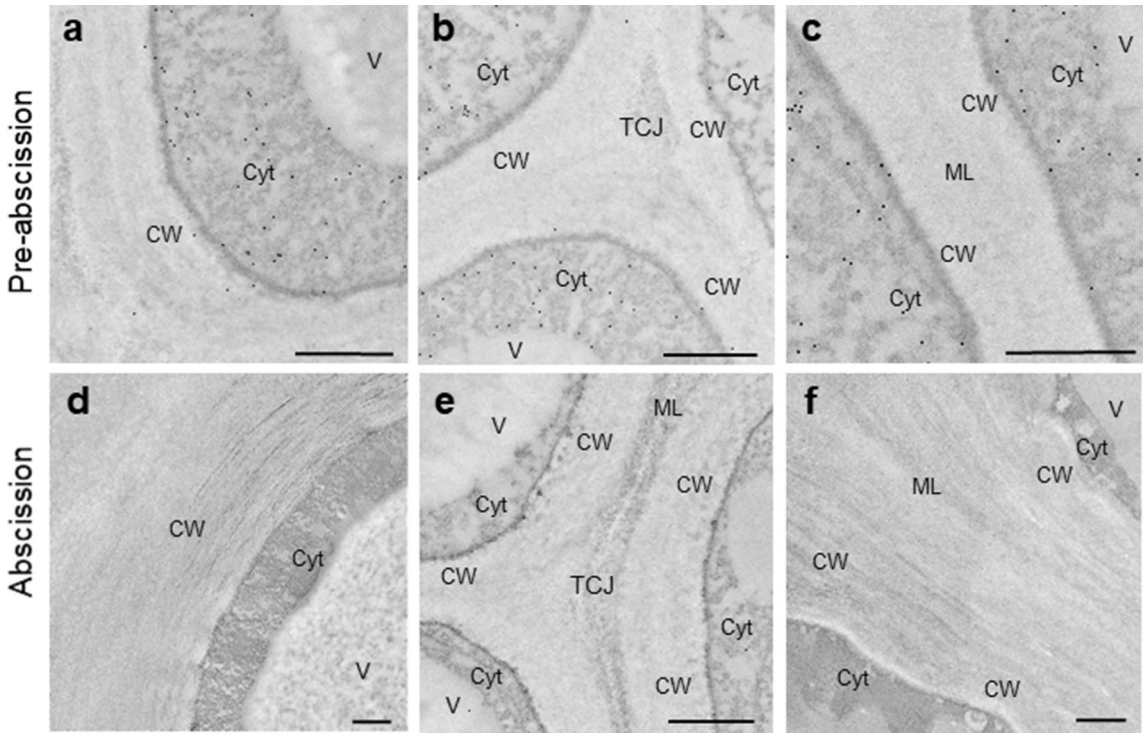

Fig. 5 Immunolocalization of extensin epitope (JIM19) in the AZ cells during ripe-fruit abscission in olive (*Olea europaea* L. cultivar 'Picual'). Transmission electron micrographs of cell junctions from longitudinal sections of the ripe-fruit AZ at **a**–**c** the pre-abscission (unseparated AZ cells), and **d**–**f** abscission (partially separated AZ cells) stages. *CW* cell-wall, *cyt* cytoplasm, *ML* middle lamella, *TCJ* tricellular junction, *v* vacuole. Scale bars 1 µm

differed during olive ripe-fruit abscission, while AZ cell-wall remodeling did not involve mannans. These results suggest that xylan and xyloglucan may contribute to olive AZ cell separation. Xylan epitopes were generally detected by LM11 antibody in the tricellular junction zones of the AZ cells, and the levels of xylan epitopes increased during ripe-fruit abscission, in parallel with the xylose and arabinose content in the carbonate extract of the AZ cell wall (Parra et al. 2020), suggesting a novel deposition of xylan and arabinoxylan in the AZ cell wall during olive ripe-fruit abscission. By contrast, our results indicate decreases in LM15 xyloglucan epitopes in AZ cell walls during olive AZ cell separation, and no significant labeling from the tricellular junction zones. In this case, this decrease of xyloglucan content during olive-fruit abscission was consistent with the amount of xylose in the imidazole fraction of the AZ cell wall (Parra et al. 2020). These observations suggest that xylan has a different function from that of xyloglucan in ripe-fruit abscission, and that a lower xyloglucan level from the AZ cell wall of olive ripe-fruit during abscission may contribute by having a loosening effect on the cellulose-xyloglucan or pectin-xyloglucan network with consequences on cell-wall mechanical properties. Moreover, our immunocytochemical study showed few LM15 epitopes in AZ cell walls. Pectins may have masked the epitopes recognized by these anti-xyloglucan antibodies, as previously suggested (Marcus et al. 2008; Bowling and Vaughn 2011; Saffer 2018). It has been proposed that some subsets of xyloglucan and pectin may be covalently linked together (Popper and Fry 2008; Cornuault et al. 2018). In this context, we recently reported that natural ripe-fruit abscission is associated with an increase in highly de-esterified homogalacturonan pectins, by the detection of the LM19 homogalacturonan epitope, from the cell walls and from the tricellular junction zones of AZ in olive (Parra et al. 2020). The potential masking of cell-wall LM15 epitopes by de-esterified homogalacturonan pectins in our AZ samples need to be considered. However, our biochemical analysis of homogenized cell walls also shows many differences in composition between stages (Parra et al. 2020). Thus, our results here indicate a negative correlation between xyloglucan and xylan in the olive AZ during natural ripe-fruit abscission. We conjecture that the appearance of hemicelluloses, such as xylan, and the modification of the pectin homogalacturonan backbone structure through de-methyl-esterification appears to be one mechanism by which cell walls and middle lamella of olive-fruit AZ are prepared for enzymatic degradation to permit AZ cell separation and collapse, and subsequently AZ cell-wall restructuring.

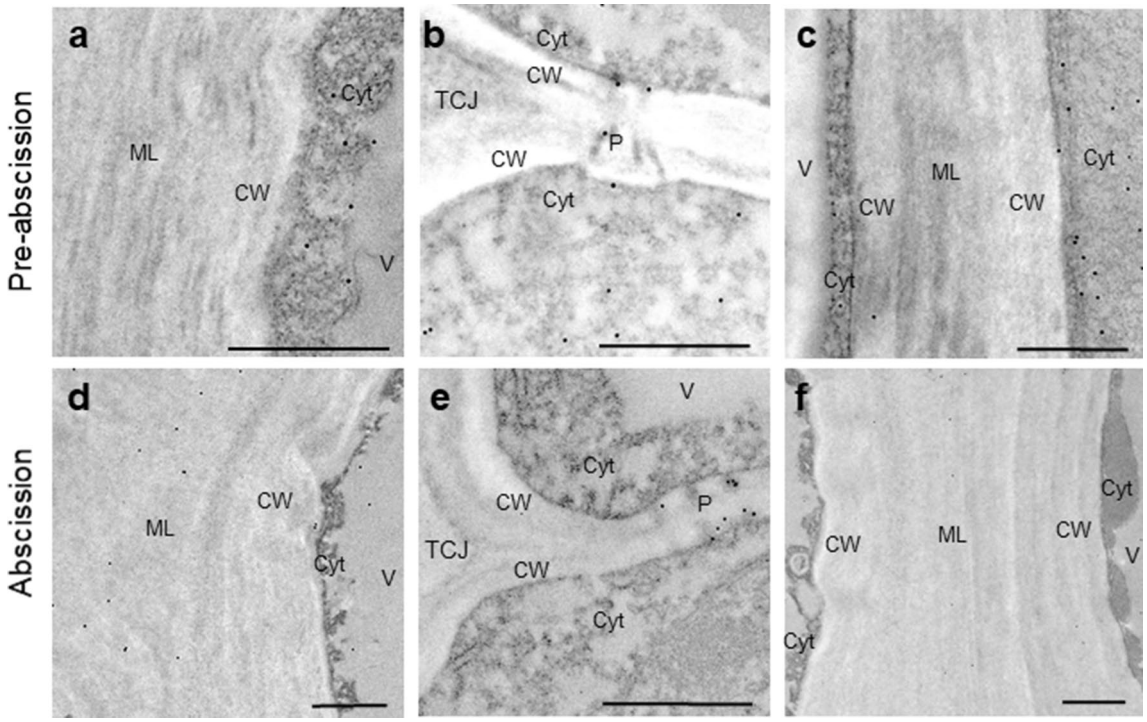

Fig. 6 Immunolocalization of callose epitope (anti-(1,3)-β-D-glucan) in the AZ cells during ripe-fruit abscission in olive (*Olea europaea* L. cultivar 'Picual'). Transmission electron micrographs of cell junctions from longitudinal sections of the fruit AZ at the **a**–**c** pre-abscission and **d**–**f** abscission stages. *CW* cell-wall, *cyt* cytoplasm, *ML* middle lamella, *TCJ* tricellular junction, *P* plasmodesmata, *v* vacuole. Scale bars 1 µm

Table 2 Quantification of immunogold labeling with anti-(1,3)-β-D-glucan antibodies during ripe-fruit abscission in olive (*Olea europaea* L. cv Picual)

	Number of gold particles			
	Cell-wall (µm^2)	Plasmodesmata (µm)	Cytoplasm (µm^2)	Vacuole (µm^2)
Anti-(1,3)-β-D-glucan				
AZ at pre-abscission stage	0.61 ± 0.12	4.25 ± 0.40	5.08 ± 0.35	1.24 ± 0.25
AZ at abscission stage	3.75 ± 0.27*	9.30 ± 0.60*	2.17 ± 0.58*	1.85 ± 0.49

Data are means of fruit AZ ± SD ($n = 15$) of three biological replicate determinations per stage and per antibody. Five fruit AZs from each tree formed a biological replicate. Statistically significant differences based on unpaired Student's t test at $p < 0.05$ are denoted by an asterisk

Few studies have focused on hemicellulose involvement in the abscission process in plant species (Lee et al. 2008; Iwai et al. 2013; Tsuchiya et al. 2015). Mannan is one of the major constituent groups of hemicellulose in the cell wall of higher plants and is widely distributed in plant tissues (Moreira and Filho 2008; Voiniciuc et al. 2018). It comprises linear or branched polymers derived from sugars such as D-mannose, D-galactose, and D-glucose (Moreira and Filho 2008; Voiniciuc et al. 2018). Recent research in our laboratory has revealed that the major sugars identified in the olive AZ cell wall were uronic acids and arabinose (Parra et al. 2020). The amount of mannose in the carbonate fraction of the AZ cell wall did not change significantly during ripe-fruit abscission, while the amount of galactose and glucose decreased during ripe-fruit abscission (Parra et al. 2020). These results are consistent with a similar distribution of mannans in the AZ cells detected by immunogold labeling during olive ripe-fruit abscission in the present study. Furthermore, this agrees with our previous results demonstrating the non-differential expression of endo-β-mannanase genes in olive AZ during ripe-fruit abscission (Gil-Amado and Gomez-Jimenez 2013), and with those from Yan et al. (2012), who reported that soybean endo-β-mannanase GmMAN1 was not associated with leaf abscission. In this context, the mannan-degrading enzyme systems, such as β-mannanase, do not play a key role in organ abscission process. Conversely, this contrasts with genes annotated as XTH, in which nine members of this family

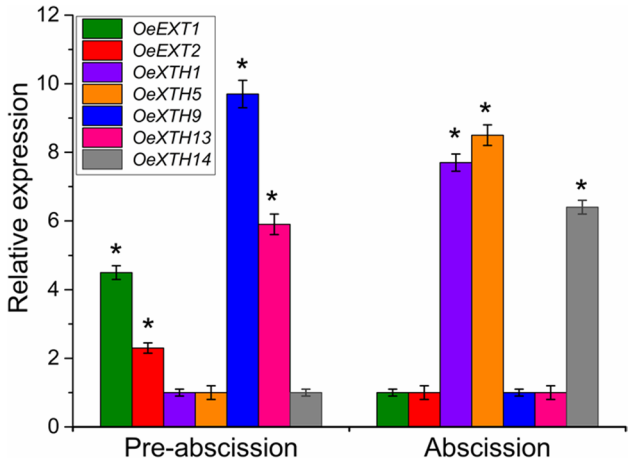

Fig. 7 Gene expression of *OeEXT1*, *OeEXT2*, *OeXTH1*, *OeXTH5*, *OeXTH9*, *OeXTH13* and *OeXTH14* mRNAs in the AZ during olive ripe-fruit abscission. Total RNAs were isolated from AZ at two different stages (pre-abscission and abscission) during fruit AZ cell separation. Data are the means ± SD of three biological replicates with three technical repeats each and were obtained by qRT-PCR normalized against *Olea europaea* ubiquitin. Statistically significant differences based on unpaired Student's *t* test at $p < 0.05$ are denoted by an asterisk

show a abscission-related differential expression in the fruit AZ, suggesting a more important role for members of the XTH family in abscission-associated cell-wall changes (Gil-Amado and Gomez-Jimenez 2013). Although further studies will require to elucidate how the protein levels and the enzyme activity of β-mannanase are regulated during olive-fruit abscission, our immunological analysis suggests that mannan in the AZ may not be depolymerized during olive-fruit abscission.

To date, the distribution of xylan and xyloglucan have been analyzed only in poinsettia and tomato during floral and fruit abscission (Lee et al. 2008; Iwai et al. 2013; Tsuchiya et al. 2015). Previous work has indicated the occurrence of xylan and xyloglucan epitopes in the cell walls of the AZ at a late stage of floral abscission in poinsettia (Lee et al., 2008). A similar increase in xyloglucan epitopes detected via immunohistochemistry has been reported in the tomato AZ during floral abscission, but no deposition of cell-wall polysaccharides was observed in the AZ during tomato ripe-fruit abscission (Iwai et al. 2013). However, our data show that the changes in the hemicellulose composition of cell walls of the olive-fruit AZ differ from those reported in the leaf petiole AZs of poinsettia (Lee et al. 2008) and impatiens (Bowling and Vaughn 2011), and in the flower-petiole AZ of tomato (Iwai et al. 2013; Tsuchiya et al. 2015). The reason for this variation between plant organs remains unclear. This discrepancy may be related to the fact that the AZ cell-wall remodeling is brought about by suites of hemicellulose-degrading enzymes, with varying cocktails acting in different plant organs and species. A wide range of hemicellulose-degrading enzymes are reportedly associated with abscission (Roberts et al. 2002; Meir et al. 2010; Sun and van Nocker 2010; Zhu et al. 2011; Corbacho et al. 2013; Gil-Amado and Gomez-Jimenez 2013; Kim et al. 2015, 2019; Li et al. 2015; Glazinska et al. 2017; Xie et al. 2018). Xyloglucan degradation is a central factor in wall modification that occurs during transient wall loosening in expanding cells or in terminal wall degradation during fruit ripening and organ abscission (Rose and Bennet 1999; Rose et al. 2002, 2003; Roberts et al. 2002; Tucker et al. 2007; Cai and Lashbrook 2008; Takizawa et al. 2014; Tsuchiya et al. 2015). XTHs have dual activities and can strengthen or loosen cell walls in different contexts (Rose et al. 2002; Eklöf and Brumer 2010). It has been proposed that some XTHs catalyze a type of cell-wall loosening that leads to extension both by cutting and restructuring the existing wall-bound xyloglucans (Rose et al. 2002; Eklöf and Brumer 2010). Here, we show that, consistent with the low xyloglucan content found in the olive AZ at the abscission stage, the process of ripe-fruit separation in olive is closely associated with the differential expression of five *XTH* genes (*OeXTH1*, *OeXTH5, OeXTH9*, *OeXTH13,* and *OeXTH14).* Although the role of individual XTHs is unknown, our results suggest that XTH enzymes may be required to allow abscission-related changes in the cell walls of olive-fruit AZ. Olive ripe-fruit abscission induced the expression of *OeXTH1*, *OeXTH5*, and *OeXTH14*, whereas *OeXTH9* and *OeXTH13* expression decreased in the ripe-fruit AZ during AZ cell separation. These results suggest that the role of *OeXTH9* and *OeXTH13* in the AZ are related to the maintenance of the structural integrity of the cell wall, and the decrease in *OeXTH9* and *OeXTH13* expression during olive AZ cell separation may contribute to cell-wall loosening, which is regulated through different XTH genes, such as *OeXTH1*, *OeXTH5*, and *OeXTH14*. These XTH genes may have hydrolase and endotransglucosylase activity in olive-fruit AZ. This agrees with our previous results in which we demonstrated the down-regulation of *CmXTH13* gene in the AZ during late induction of melon ripe-fruit abscission, suggesting that *CmXTH13* action may not be important for wall restructuring after AZ cell separation (Corbacho et al. 2013). The expression of other *XTH* genes has been previously shown to be associated with abscission in soybean (*XET1* and *XET2* Tucker et al. 2007), citrus (*XTH1* and *XTH2*, Agusti et al. 2008; *XTH16*, *XTH24*, and *XTH28*, Merelo et al. 2017), Arabidopsis (*XTH7*, *XTH12*, *XTH14* and *XTH28*, Cai and Lashbrook 2008), tomato (*XET-BR1*, Meir et al. 2010; Tsuchiya et al. 2015), rose (Singh et al. 2011), litchi (Li et al. 2015), and yellow lupine (Glazinska et al. 2017). In Arabidopsis floral organ abscission, XTHs are active in AZs over all stages from pre-pollination to organ shed (Cai and Lashbrook 2008). The

expression of *XTH12* and *XTH28* increased continually in the stamen AZ during flower development, while expression of *XTH14* and *XTH7* decreased during early flower development stages and increased during the progress of stamen abscission (Cai and Lashbrook 2008). In tomato, *XET-BR1* gene expression increased significantly and remained high in the AZ after flower removal (Meir et al. 2010). Likewise, the cell-wall remodeling through rearrangement of the cell-wall xyloglucans by the XET action of one to several XTHs might be a major determinant in rose-petal abscission (Singh et al. 2011). Altogether, the analysis has identified several candidate genes/proteins possibly involved in the AZ cell-wall modifications observed during natural ripe olive-fruit abscission. Experiments are still needed to elucidate how the protein levels and the enzyme activity of XTH are regulated during olive-fruit abscission. Based on immunological and expression analyses, we hypothesize that the differences in the bulk of hydrolases and cell-wall hemicellulose remodeling proteins between AZs may reflect differences in cell-wall hemicellulose composition of the AZ in different plant organs and species.

Various proteins involved in the reconstruction of cell walls remodel the chemical structure and interactions of cell-wall pectin, hemicelluloses, and cellulose in the cell wall (Wolf et al. 2012; Voiniciuc et al. 2018). Extensins constitute one of the classes of plant structural cell-wall proteins (Lamport et al. 2011; Liu et al. 2016), but the role in abscission played by these cell-wall proteins has received little attention. No reports are available on the distribution of extensin in the AZ, using immunomicroscopic methods, during organ abscission. Here, we found that natural ripe-fruit abscission is associated with an extensin protein loss, by the detection of the JIM19 extensin epitope, from the cell wall and especially from the cytoplasm of the AZ cells in olive. The reason for extensin absence in olive AZ cell at the abscission stage is not clear. Adhesion changes regulated by different cell-wall ions may modulate the interactions of AGPs and/or extensins in specific biological process (Tan et al. 2018). In the present study, our data suggest that a loss of extensin proteins during ripe-fruit abscission could be a mechanism to facilitate AZ cell-wall loosening and AZ cell separation. Extensins occur in multigene families and each member may be expressed in a tissue-specific manner and likely fulfills a different function (Lamport et al. 2011; Liu et al. 2016; Showalter and Basu 2016; Doll et al. 2020). In the present study, our data reveal the down-regulation of two genes encoding extensin (*OeEXT1* and *OeEXT2*) in olive AZ during ripe-fruit abscission, verifying our pyrosequencing data (Gil-Amado and Gomez-Jimenez 2013), and supporting the contention that these transcripts are reduced in the olive AZ throughout abscission. These results suggest that extensin in the olive-fruit AZ could be involved in the maintenance of the structural integrity of the cell wall, and the decrease in *OeEXT1* and *OeEXT2* expression may contribute to olive-fruit AZ cell separation. However, these results differ significantly from those of other plant species during ripe-fruit abscission; an accumulation of *EXT1-EXT4* expression has been found in the AZ during both the early and late induction of ripe-fruit abscission in melon (Corbacho et al. 2013), as also indicated during floral organ abscission in Arabidopsis (Merkouropoulos and Shirsat 2003). The *EXT1-EXT4* gene is induced by wounding, and by a range of stimuli such as abscisic acid (ABA), jasmonic-acid (JA), and salicylic-acid (SA) (Merkouropoulos and Shirsat 2003). Thus, our data reveal a relationship between extensin protein/gene expression and ripe-fruit abscission in olive, indicating that fruit abscission process in olive is accompanied by the loss of extensin proteins epitopes and reduction of *OeEXT1* and *OeEXT2* gene expression in the AZ cells.

Callose stabilizes membranes, providing a spreading force for microtubules, but also acts as a developmental regulator of symplasmic continuity (Chen and Kim 2009). Its exact role in abscission is still unknown. In the present study, our data imply that callose deposition especially from the plasmodesmatal connections on the AZ cell wall can exert a positive effect on wall remodeling during olive ripe-fruit abscission, or that the high callose level in the AZ cell walls enhances abscission signaling in olive. We have previously reported that, during olive ripe-fruit abscission, the down-regulation of a gene encoding one callose synthase and up-regulation of one gene encoding β-1,3-glucanase in the AZ (Gil-Amado and Gomez-Jimenez 2013). By contrast, two callose synthases were preferentially expressed in the petiolar cortical cells during citrus leaf ethylene-promoted abscission (Agusti et al. 2009). One of the functions of the cell wall is to constitute a defensive barrier to prevent the penetration of pathogens into the plant tissues (Kruger et al. 2002). Callose is deposited between the plasmalemma and the cell wall in close proximity to the site of invasion of the pathogen. We might envisage that the deposition of callose in the AZ is a protective response against the foreseeable attack of pathogens when fruits are finally detached. However, it has been shown that callose participates in fine-tuning the opening/closure dynamics of the plasmodesmata (Sun et al. 2019) and that AZ cells are connected by abundant plasmodesmata pores (Sexton and Roberts 1982). Thus, it would be reasonable to propose that abscission activation promotes callose deposition in plasmodesmata to stop cell-to-cell communication in the fruit AZ and to other surrounding cell types. It has been reported that there was callose deposition in leaf petiole AZs during abscission alongside lignin deposition suggesting that it may be necessary to prevent water loss after abscission (Poovaiah 1974; Jaffe and Goren 1988). Based on the above reasoning and our data, we suggest that, for the AZ cell walls of olive ripe-fruit, an increase in the occurrence of callose in or around

plasmodesmata can be associated with the isolation of AZs from the cellular environment during abscission.

Conclusion

The results presented here, concerning the distribution of extensin and hemicellulose epitopes in the AZ of olive ripe-fruit, indicate some spatio–temporal similarities and differences during AZ cell separation. The immunocytochemical study using antibodies specific for extensin and hemicelluloses combined with gene expression study provide new insight on level and subcellular distribution of different types of AZ cell-wall components during fleshy-fruit abscission. This work reveals a mechanism for enabling AZ cell separation, which was associated with a loss of extensin and lower xyloglucan level, with novel deposition of xylan and callose, as well as with a significant up-regulation of genes encoding XTH enzyme involved in cell-wall loosening in the AZ during olive ripe-fruit abscission. Therefore, the complementary pattern of increased xylan labeling density and the lack of extensin detection in the olive AZ were related to AZ cell separation, while no differences in the distribution of mannans were found in olive AZ cell during ripe-fruit abscission. These results point to new questions about the role of extensin and hemicelluloses in cell separation. This is the first available immunocytochemical study concerning the temporal degradation of cell-wall extensin protein and hemicelluloses in the AZ at the subcellular level.

Author contribution statement MCG-J designed the research. RP performed the experiments. MCG-J and RP analyzed the data. MCG-J wrote the manuscript.

Acknowledgements This work was supported by grants from the Spanish Ministry of Economy and Competitiveness (AGL2014-52194-R and RTI2018-097244-B-I00), the Junta of Extremadura (Spain) and the European Regional Development Fund (IB18075). The authors thank J. L. Grosson for free access to the plant material and D. Nesbitt for correcting the English. They are grateful to the Research Support Service of University of Extremadura for its contribution to this work.

References

Agustí J, Merelo P, Cercós M, Tadeo FR, Talón M (2008) Ethylene-induced differential gene expression during abscission of citrus leaves. J Exp Bot 59:2717–2733

Agustí J, Merelo P, Cercos M, Tadeo FR, Talón M (2009) Comparative transcriptional survey between laser-microdissected cells from laminar abscission zone and petiolar cortical tissue during ethylene-promoted abscission in citrus leaves. BMC Plant Biol 9:127

Barranco D, Arquero O, Navarro C, Rapoport HF (2004) Monopotassium phosphate for olive fruit abscission. HortScience 39:1313–1314

Bartolini S, Cantini C, Vitagliano C (1993) Olive fruit abscission: anatomical observations following application of ethylene-releasing compound. Acta Hortic 329:249–251

Belfield EJ, Ruperti B, Roberts JA, McQueen-Mason S (2005) Changes in expansin activity and gene expression during ethylene-promoted leaflet abscission in *Sambucus nigra*. J Exp Bot 56:817–823

Bleecker AB, Patterson SE (1997) Last exit: senescence, abscission, and meristem arrest in *Arabidopsis*. Plant Cell 9:1169–1179

Bouton S, Leboeuf E, Mouille G, Leydecker MT, Talbotec J, Granier F et al (2002) QUASIMODO1 encodes a putative membrane-bound glycosyltransferase required for normal pectin synthesis and cell adhesion in *Arabidopsis*. Plant Cell 14:2577–2590

Bowling AJ, Vaughn KC (2011) Leaf abscission in impatiens (*Balsaminaceae*) is due to loss of highly de-esterified homogalacturonans in the middle lamellae. Am J Bot 98:619–629

Burns J, Ferguson L, Glozer K, Krueger WH, Rosecrance RC (2008) Screening fruit loosening agents for black ripe processed table olives. HortScience 43:1449–1453

Caffall KH, Mohnen D (2009) The structure, function, and biosynthesis of plant cell-wall pectic polysaccharides. Carbohydr Res 344:1879–1900

Cai S, Lashbrook CC (2008) Stamen abscission zone transcriptome profiling reveals new candidates for abscission control: enhanced retention of floral organs in transgenic plants overexpressing *Arabidopsis* ZINC FINGER PROTEIN2. Plant Physiol 146:1305–1321

Carpita NC, Gibeaut DM (1993) Structural models of primary cell-walls in flowering plants: consistency of molecular structure with the physical properties of walls during growth. Plant J 3:1–30

Chaikumpollert O, Methacanon P, Suchiva K (2004) Structural elucidation of hemicelluloses from Vetiver grass. Carbohydr Polym 57:191–196

Chen XY, Kim JY (2009) Callose synthesis in higher plants. Plant Signal Behav 4:489–492

Cho SK, Larue CT, Chevalier D, Wang H, Jinn TL, Zhang S, Walker JC (2008) Regulation of floral organ abscission in *Arabidopsis thaliana*. PNAS 105:15629–15634

Corbacho J, Romojaro F, Pech J-C, Latché A, Gomez-Jimenez MC (2013) Transcriptomic events involved in melon mature-fruit abscission comprise the sequential induction of cell-wall degrading genes coupled to a stimulation of endo and exocytosis. PLoS ONE 8:e58363

Cornuault V, Posé S, Knox JP (2018) Disentangling pectic homogalacturonan and rhamnogalacturonan-I polysaccharides: evidence for sub-populations in fruit parenchyma systems. Food Chem 246:275–285

Cosgrove DJ (1997) Assembly and enlargement of the primary cell-wall in plants. Annu Rev Cell Dev Bi 13:171–201

Coupe SA, Taylor JE, Isaac PG, Roberts JA (1993) Identification and characterization of a proline-rich mRNA that accumulates during pod development in oilseed rape (*Brassica napus* L.). Plant Mol Biol 23:1223–1232

Doll NM, Bovio S, Gaiti A, Marsollier A-C, Chamot S, Moussu S, Widiez T, Ingram G (2020) The endosperm-derived embryo sheath is an anti-adhesive structure that facilitates cotyledon emergence during germination in *Arabidopsis*. Curr Biol 30:909–915

Eklöf JM, Brumer H (2010) The XTH gene family: an update on enzyme structure, function, and phylogeny in xyloglucan remodeling. Plant Physiol 153:456–466

Gil-Amado JA, Gomez-Jimenez MC (2013) Transcriptome analysis of mature fruit abscission control in olive. Plant Cell Physiol 54:244–269

Glazinska P, Wojciechowski W, Kulasek M, Glinkowski W, Marciniak K, Klajn N, Kesy J, Kopcewicz J (2017) De novo transcriptome profiling of flowers, flower pedicels and pods of *Lupinus luteus*

(*yellow lupine*) reveals complex expression changes during organ abscission. Front Plant Sci 8:641

Gomez-Jimenez MC, Paredes MA, Gallardo M, Sanchez-Calle IM (2010a) Mature fruit abscission is associated with up-regulation of polyamine metabolism in the olive abscission zone. J Plant Physiol 167:1432–1441

Gomez-Jimenez MC, Paredes MA, Gallardo M, Fernandez-Garcia N, Olmos E, Sanchez-Calle IM (2010b) Tissue-specific expression of olive *S*-adenosyl methionine decarboxylase and spermidine synthase genes and polyamine metabolism during flower opening and early fruit development. Planta 232:629–647

Hayashi T, Kaida R (2011) Functions of xyloglucan in plant cells. Mol Plant 4:17–24

Hervé C, Rogowski A, Gilbert HJ, Knox JP (2009) Enzymatic treatments reveal differential capacities for xylan recognition and degradation in primary and secondary plant cell-walls. Plant J 58:413–422

Iwai H, Terao A, Satoh S (2013) Changes in distribution of cell-wall polysaccharides in floral and fruit abscission zones during fruit development in tomato (*Solanum lycopersicum*). J Plant Res 126:427–437

Jaffe MJ, Goren R (1988) Deposition of callose in relation to abscission of citrus leaves. Physiol Plant 72:329–336

Kim J, Sundaresan S, Philosoph-Hadas S, Yang R, Meir S, Tucker ML (2015) examination of the abscission-associated transcriptomes for soybean, tomato, and Arabidopsis highlights the conserved biosynthesis of an extensible extracellular matrix and boundary layer. Front Plant Sci 6:1109

Kim J, Chun J-P, Tucker ML (2019) Transcriptional regulation of abscission zones. Plants 8:154

Kruger WM, Carver TLW, Zeyen RJ (2002) Effects of inhibiting phenolic biosynthesis on penetration resistance of barley isolines containing seven powdery mildew resistance genes or alleles. Physiol Mol Plant Pathol 61:41–51

Lamport DT, Kieliszewski MJ, Chen Y, Cannon MC (2011) Role of the extensin superfamily in primary cell-wall architecture. Plant Physiol 156:11–19

Lee Y, Derbyshire P, Knox JP, Hvoslef-Eide AK (2008) Sequential cell-wall transformations in response to the induction of a pedicel abscission event in *Euphorbia pulcherrima* (poinsettia). Plant J 54:993–1003

Lee Y, Ayeh KO, Ambrose M, Hvoslef-Eide AK (2016) Immunolocalization of pectic polysaccharides during abscission in pea seeds (*Pisum sativum* L.) and in abscission less def pea mutant seeds. BMC Res Notes 9:427

Levesque-Tremblay G, Pelloux J, Braybrook SA, Müller K (2015) Tuning of pectin methylesterification: consequences for cell-wall biomechanics and development. Planta 242:791–811

Li C, Wang Y, Ying P, Ma W, Li J (2015) Genome-wide digital transcript analysis of putative fruitlet abscission related genes regulated by ethephon in litchi. Front Plant Sci 6:502

Liepman AH, Nairn CJ, Willats WGT, Sørensen I, Roberts AW, Keegstra K (2007) Functional genomic analysis supports conservations of function among cellulose synthase-like A gene family members and suggests diverse roles of mannans in plants. Plant Physiol 143:1881–1893

Liu X, Wolfe R, Welch LR, Domozych DS, Popper ZA, Showalter AM (2016) Bioinformatic Identification and Analysis of Extensins in the Plant Kingdom. PLoS ONE 11:e0150177

Marcus SE, Verhertbruggen Y, Hervé C, Ordaz-Ortiz JJ, Farkas V, Pedersen HL, Willats WGT, Knox JP (2008) Pectic homogalacturonan masks abundant sets of xyloglucan epitopes in plant cell-walls. BMC Plant Biol 8:60

Marcus SE, Blake AW, Benians TA, Lee KJ, Poyser C, Donaldson L, Leroux O, Rogowski A, Petersen HL, Boraston A, Gilbert HJ, Willats WG, Knox JP (2010) Restricted access of proteins to mannan polysaccharides in intact plant cell-walls. Plant J 64:191–203

McCartney L, Knox JP (2002) Regulation of pectic polysaccharide domains in relation to cell development and cell properties in the pea testa. J Exp Bot 53:707–713

McCartney L, Marcus SE, Knox JP (2005) Monoclonal antibodies to plant cell-wall xylans and arabinoxylans. J Histochem Cytochem 53:543–546

McManus MT (2008) Further examination of abscission zone cells as ethylene target cells in higher plants. Ann Bot 101:285–292

Meikle PJ, Bonig I, Hoogenraad NJ, Clarke AE, Stone BA (1991) The location of (1→3)-β-glucans in the walls of pollen tubes of Nicotiana alata using a (1→3)-β-glucan-specific monoclonal antibody. Planta 185:1–8

Meir S, Philosoph-Hadas S, Sundaresan S, Selvaraj KSV, Burd S, Ophir R et al (2010) Microarray analysis of the abscission-related transcriptome in the tomato flower abscission zone in response to auxin depletion. Plant Physiol 154:1929–1956

Meir S, Philosoph-Hadas S, Riov J, Tucker ML, Patterson SE, Roberts JA (2019) Re-evaluation of the ethylene-dependent and -independent pathways in the regulation of floral and organ abscission. J Exp Bot 70:1461–1467

Merelo P, Agustí J, Arbona V, Costa ML, Estornell LH, Gómez-Cadenas A et al (2017) Cell-wall remodeling in abscission zone cells during ethylene-promoted fruit abscission in citrus. Front Plant Sci 8:126

Merkouropoulos G, Shirsat AH (2003) The unusual Arabidopsis extensin gene Atext1 is expressed throughout plant development and is induced by a variety of biotic and abiotic stresses. Planta 217:356–366

Moreira LRS, Filho EXF (2008) An overview of mannan structure and mannan-degrading enzyme systems. Appl Microbiol Biotechnol 79:165–178

Mortimer JC, Blanc NF, Yu X, Anders N, Tryfona T, Sorieul M, Ng YZ, Zhang Z, Stott K, Dupree P (2015) An unusual xylan in Arabidopsis primary cell-walls is synthesised by GUX3, IRX9L, IRX10L and IRX14. Plant J 83:413–426

Niederhuth CE, Cho SK, Seitz K, Walker JC (2013) Letting go is never easy: abscission and receptor-like protein kinases. J Integr Plant Biol 55:1251–1263

Olmos E, García De La Garma J, Gomez-Jimenez MC, Fernandez-Garcia N (2017) Arabinogalactan proteins are involved in salt-adaptation and vesicle trafficking in tobacco by-2 cell cultures. Front Plant Sci 8:1092

O'Neill MA, York WS (2003) The composition and structure of plant primary cell-wall. In: Rose JKC (ed) The plant cell-wall. Blackwell Publishing, Oxford

Palmer R, Cornuault V, Marcus SE, Knox JP, Shewry PR, Tosi P (2015) Comparative in situ analyses of cell-wall matrix polysaccharide dynamics in developing rice and wheat grain. Planta 241:669–685

Parra R, Paredes MA, Sanchez-Calle IM, Gomez-Jimenez MC (2013) Comparative transcriptional profiling analysis of olive ripe-fruit pericarp and abscission zone tissues shows expression differences and distinct patterns of transcriptional regulation. BMC Genomics 9:866

Parra R, Paredes MA, Labrador J, Nunes C, Coimbra MA, Fernandez-Garcia N, Olmos E, Gallardo M (2020) Gomez-Jimenez MC (2020) Cell wall composition and ultrastructural immunolocalization of pectin and arabinogalactan protein during *Olea europaea* L. fruit abscission. Plant Cell Physiol 61:814–825

Parra-Lobato MC, Gomez-Jimenez MC (2011) Polyamine-induced modulation of genes involved in ethylene biosynthesis and signalling pathways and nitric oxide production during olive mature fruit abscission. J Exp Bot 62:4447–4465

Parra-Lobato MC, Paredes MA, Labrador J, Saucedo-García M, Gavilanes-Ruiz M, Gomez-Jimenez MC (2017) Localization of

sphingolipid enriched plasma membrane regions and long-chain base composition during mature-fruit abscission in olive. Front Plant Sci 8:1138
Patharkar OR, Walker JC (2018) Advances in abscission signaling. J Exp Bot 69:733–740
Patterson SE (2001) Cutting loose. Abscission and dehiscence in Arabidopsis. Plant Physiol 126:494–500
Pauly M, Keegstra K (2016) Biosynthesis of the plant cell-wall matrix polysaccharide xyloglucan. Annu Rev Plant Biol 67:235–259
Périn C, Gomez-Jimenez MC, Hagen L, Dogimont C, Pech JC, Latche A et al (2002) Molecular and genetic characterization of a non-climacteric phenotype in melon reveals two loci conferring altered ethylene response in fruit. Plant Physiol 129:300–309
Poovaiah B (1974) Formation of callose and lignin during leaf abscission. Am J Bot 61:829–834
Popper ZA, Fry SC (2008) Xyloglucan-pectin linkages are formed intra-protoplasmically, contribute to wall-assembly, and remain stable in the cell wall. Planta 227:781–794
Prakash R, Hallett IC, Wong SF, Johnston SL, O'Donoghue EM, McAtee PA, Seal AG, Atkinson RG, Schröder R (2017) Cell separation in kiwifruit without development of a specialised detachment zone. BMC Plant Biol 17:86
Roberts JA, Elliott KA, Gonzalez-Carranza ZH (2002) Abscission, dehiscence, and other cell separation processes. Annu Rev Plant Biol 53:131–158
Roongsattham P, Morcillo F, Fooyontphanich K, Jantasuriyarat C, Tragoonrung S, Amblard P et al (2016) Cellular and pectin dynamics during abscission zone development and ripe fruit abscission of the monocot oil palm. Front Plant Sci 7:540
Rose JK, Bennett AB (1999) Cooperative disassembly of the cellulose-xyloglucan network of plant cell-walls: parallels between cell expansion and fruit ripening. Trends Plant Sci 4:176–183
Rose JKC, Braam J, Fry SC, Nishitani K (2002) The XTH family of enzymes involved in xyloglucan endotransglucosylation and endohydrolysis: current perspectives and a unifying nomenclatura. Plant Cell Physiol 43:1421–1435
Rose JKC, Catalá C, Gonzalez-Carranza ZH, Roberts J (2003) Plant cell-wall disassembly. In: Rose JKC (ed) The plant cell-wall. Blackwell Publishing, Oxford, pp 264–324
Saffer AM (2018) Expanding roles for pectins in plant development. J Integr Plant Biol 60(10):910–923
Saha P, Ray T, Tang Y, Dutta I, Evangelous NR, Kieliszewski MJ, Chen Y, Cannon MC (2013) Self-rescue of an EXTENSIN mutant reveals alternative gene expression programs and candidate proteins for new cell wall assembly in Arabidopsis. Plant J 75(1):104–116
Scheller HV, Ulvskov P (2010) Hemicelluloses. Annu Rev Plant Biol 61:263–289
Seifert GJ, Roberts K (2007) The biology of arabinogalactan proteins. Annu Rev Plant Biol 58:137–161
Sexton R, Roberts JA (1982) Cell biology of Abscission. Annu Rev Plant Biol 33:133–162
Showalter AM, Basu D (2016) Extensin and arabinogalactan-protein biosynthesis: glycosyltransferases, research challenges, and biosensors. Front Plant Sci 7:814
Singh AP, Tripathi SK, Nath P, Sane AP (2011) Petal abscission in rose is associated with the differential expression of two ethylene-responsive xyloglucan endotransglucosylase/hydrolase genes, *RbXTH1* and *RbXTH2*. J Exp Bot 62:5091–5103
Stenvik GE, Butenko MA, Urbanowicz BR, Rose JK, Aalen RB (2006) Overexpression of INFLORESCENCE DEFICIENT IN ABSCISSION activates cell separation in vestigial abscission zones in Arabidopsis. Plant Cell 18:1467–1476
Sun L, van Nocker S (2010) Analysis of promoter activity of members of the PECTATE LYASE-LIKE (PLL) gene family in cell separation in Arabidopsis. BMC Plant Biol 10:152
Sun Y, Huang D, Chen X (2019) Dynamic regulation of plasmodesmatal permeability and its application to horticultural research. Hortic Res 6:47
Takizawa A, Hyodo H, Wada K, Ishii T, Satoh S, Iwai H (2014) Regulatory specialization of xyloglucan (XG) and glucuronoarabinoxylan (GAX) in pericarp cell-walls during fruit ripening in tomato (*Solanum lycopersicum*). PLoS ONE 9:e89871
Tan L, Tees D, Qian J, Kareem S, Kieliszewski MJ (2018) Intermolecular interactions between glycomodules of plant cell-wall arabinogalactan-proteins and extensins. Cell Surf 1:25–33
Thompson J, Higgins D, Gibson T (1994) CLUSTAL W: improving the sensitivity of progressive multiple sequence through sequence weighting, position-specific gap penalties and weight matrix choice. Nucl Acids Res 22:4673–4680
Tranbarger TJ, Tadeo FR (2020) Diversity and functional dynamics of fleshy fruit abscission zones. Annu Plant Rev 3:151–214
Tsuchiya M, Satoh S, Iwai H (2015) Distribution of XTH, expansin, and secondary-wall-related CesA in floral and fruit abscission zones during fruit development in tomato (*Solanum lycopersicum*). Front Plant Sci 6:323
Tucker ML, Burke AM, Murphy CA, Thai VK, Ehrenfried ML (2007) Gene expression profiles for cell-wall-modifying proteins associated with soybean cyst nematode infection, petiole abscission, root tips, flowers, apical buds, and leaves. J Exp Bot 58:3395–3406
Uheda E, Nakamura S (2000) Abscission of Azolla branches induced by ethylene and sodium azide. Plant Cell Physiol 41:1365–1372
Voiniciuc C, Pauly M, Usadel B (2018) Monitoring polysaccharide dynamics in the plant cell-wall. Plant Physiol 176:2590–2600
Wolf S, Mauille G, Pelloux J (2009) Homogalacturonan methylesterification and plant development. Mol Plant 2:851–860
Wolf S, Hématy K, Höfte H (2012) Growth control and cell-wall signaling in plants. Annu Rev Plant Biol 63:381–407
Xie RJ, Deng L, Jing L, He SL, Ma YT, Yi SL, Zheng YQ, Zheng L (2013) Recent advances in molecular events of fruit abscission. Biol Plant 57:201–209
Xie R, Ge T, Zhang J, Pan X, Ma Y, Yi S, Zheng Y (2018) The molecular events of IAA inhibiting citrus fruitlet abscission revealed by digital gene expression profiling. Plant Physiol Bioch 130:192–204
Yan M, Zhang Y, Guo W, Wang X (2012) Soybean endo-b-mannanase GmMAN1 is not associated with leaf abscission, but might be involved in the response to wounding. PLoS ONE 7(11):e49197
Zdanio M, Boron AK, Balcerowicz D, Schoenaers S, Markakis MN, Mouille G, Pintelon I, Suslov D, Gonneau M, Höfte H, Vissenberg K (2020) The proline-rich family protein EXTENSIN33 is required for etiolated *Arabidopsis thaliana* hypocotyl growth. Plant Cell Physiol 61:1191–1203
Zhu H, Dardick C, Beers E, Callanhan A, Xia R, Yuan R (2011) Transcriptomics of shading-induced and NAA-induced abscission in apple (*Malus domestica*) reveals a shared pathway involving reduced photosynthesis, alterations in carbohydrate transport and signaling and hormone crosstalk. BMC Plant Biol 11:138